Corrosion Science 78 (2014) 162–171

Contents lists available at ScienceDirect

Corrosion Science

journal homepage: www.elsevier.com/locate/corsci

Experimental and numerical studies of effectiveness of cathodic protection at corrosion defects on pipelines

L.Y. Xu, Y.F. Cheng *

Department of Mechanical & Manufacturing Engineering, University of Calgary, Calgary, Alberta T2N 1N4, Canada

ARTICLE INFO

Article history:
Received 6 May 2013
Accepted 25 September 2013
Available online 4 October 2013

Keywords:
A. Steel
B. Modelling studies
C. Cathodic protection

ABSTRACT

In this work, the effectiveness of cathodic protection (CP) at corrosion defects on an X100 steel pipeline was investigated both experimentally and numerically. A finite element model was developed to simulate distributions of local potential and anodic/cathodic current density inside the defect. Results demonstrated that there is a non-uniform potential and current distribution at corrosion defects. The CP is shielded, at least partially, at the defect, especially at its bottom. This effect is enhanced with increasing depth and decreasing width of the defect. Empirical equations are derived to enable calculation of CP effectiveness at corrosion defects, providing industry recommendations for accurate assessment of further corrosion allowance and remaining life of pipelines in the field.

1. Introduction

There are a large number of factors that are able to affect negatively the safety and reliability of pipelines [1], such as mechanical damage introduced by manufacturing and construction, third-party factors, ground movement, and corrosion. In particular, corrosion is of great importance because the loss of the pipe wall thickness can induce a reduction of the structural reliability and hence an increase in the risk of failure [2,3]. Generally, corrosion results in several types of defect on pipe wall, such as macroscopic holes due to general corrosion occurring over a large area, corrosion pits due to localized corrosion, and cracks generated by stress corrosion cracking (SCC) [4–8]. Compared to macroscopic corrosion holes, corrosion pits and cracks usually result in a higher risk to pipelines due to their large geometrical depth, rapid propagation, and difficulty in detection.

Cathodic protection (CP), which is usually in conjunction with coatings, is generally recognized as the most effective method for corrosion prevention [9–11]. Nevertheless, its effectiveness may reduce at corrosion pits and cracks [7]. Field experiences [12] have found a significant number of corrosion defects such as pits and cracks on the external surface of cathodically protected pipelines after several years of service [13–15]. While numerical method has been used in CP design [16–18], regrettably, there has been no model to enable quantification of CP performance at various geometrical corrosion defects on pipelines. This is partially due to the experimental difficulty that the measuring probe or electrode is not accessible to the environment inside pits and cracks. Moreover, the CP effectiveness at corrosion defects such as pits and cracks has not been paid an appropriate attention. Therefore, there has been very limited work in this area that is available for reference or citation [19,20].

In this work, the effectiveness of CP at corrosion defects with varied geometries on pipelines was investigated both experimentally and numerically. A home-made potential microprobe, combined with a scanning vibrating electrode technique (SVET), was used to measure the local potential and current density as well as their distributions at artificial defects with various geometries contained on an X100 pipeline steel specimen. A finite element (FE) model was developed to simulate the anodic and cathodic current densities as a function of the defect geometry. Empirical equations were derived to enable assessment of corrosion and localized corrosion of pipelines under CP. The implications on pipeline operation and the integrity maintenance were discussed.

2. Experimental

2.1. Materials and solutions

Specimen used in this work was cut from a sheet of X100 steel pipe wall along the circumferential direction, with a chemical composition shown in Table 1. The specimen was machined into a rectangular solid that contained 5 cylindrical holes with different diameters but with an identical penetration to simulate corrosion defects on the pipe wall, as shown in Fig. 1. While the big defects simulate those generated by general corrosion, the small ones are like crevices and may have local changes in the chemistry in the field. Moreover, this work was focused on defects which grow transversely, i.e., along the pipe wall thickness direction. Those

* Corresponding author. Tel.: +1 403 220 3693; fax: +1 403 282 8406.
E-mail address: fcheng@ucalgary.ca (Y.F. Cheng).

0010-938X/$ - see front matter © 2013 Elsevier Ltd. All rights reserved.
http://dx.doi.org/10.1016/j.corsci.2013.09.011

Table 1
Chemical composition of X100 steel (wt%).

C	Mn	S	Si	P	Ni	Cr	Mo	V	Cu	Al
0.07	1.76	0.005	0.1	0.018	0.154	0.016	0.2	0.005	0.243	0.027

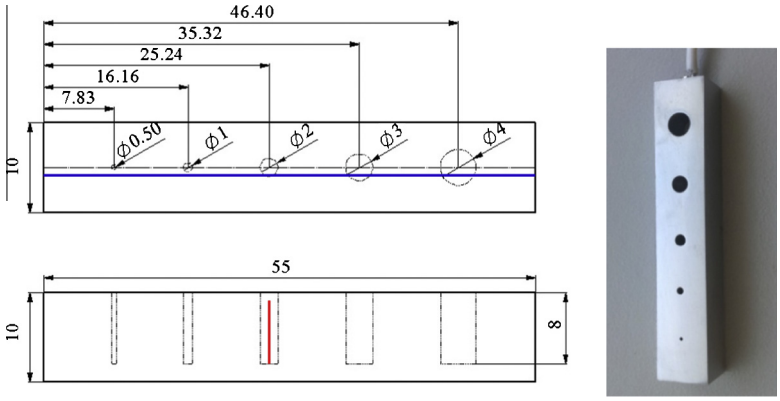

Fig. 1. Geometry of X100 steel specimen with various artificial defects (unit: mm).

defects that are part of external coating were not included. Prior to test, the specimen was ground up to 1000 grit silicon carbide paper, and then rinsed with deionized water and degreased in acetone.

The test solution was a near-neutral pH NS4 solution, which has been used widely to simulate the electrolyte trapped under disbonded coating in the field [13]. The solution contained 0.483 g/L $NaHCO_3$, 0.122 g/L KCl, 0.181 g/L $CaCl_2{\cdot}H_2O$ and 0.131 g/L $MgSO_4{\cdot}7H_2O$, made from analytic grade reagents and ultra-pure water (18 MΩ cm in resistivity). The solution was purged continuously with 5% CO_2 balanced with N_2 gas to achieve an anaerobic and near-neutral pH condition (pH = 6.8). The gas flow was maintained throughout the test.

All tests were performed at ambient temperature (~22 °C).

2.2. Local potential and SVET measurements

The local potential and SVET measurements were performed on the steel specimen through a PAR Model 370 scanning electrochemical workstation, where a saturated calomel electrode (SCE) was used as reference electrode (RE), a platinum wire as counter electrode (CE) and the steel specimen as working electrode (WE). The details of the micro-electrochemical testing were described previously [21].

The potential distribution inside corrosion defects was measured using a home-made potential microprobe, as illustrated in Fig. 2. It was made of a platinum wire with a diameter of 0.48 mm. The surface of the platinum wire was coated with a 0.05 mm thick methyl 2-cyanoacrylate electric insulating layer, leaving a tip exposed to solution. To calibrate the platinum wire microprobe for potential measurements, its open-circuit potential vs. SCE in NS4 solution is measured and shown in Fig. 3. The microprobe showed a high stability in the solution. With help of a 3-axis motion platform of the scanning electrochemical workstation, the microprobe was able to either move over the steel electrode surface or penetrate into defects. The scanning path of the microprobe inside corrosion defect was along its central line, as marked in red[1] in Fig. 1. Measurement of potential on the electrode surface was along the horizontal line marked in blue in Fig. 1 from left to right with a total length of 55 mm. The distance between microprobe and the steel electrode was controlled precisely to be 200 μm. The size of the steel specimen would not affect the measurement result, but the distance between defects could. The distance selected in this work was appropriate to avoid the overlapping of current peaks generated at individual defect, which can be seen in the current density mapping by SVET in Results section. Moreover, upon installation of the micro-probe in the defect, a shielding effect would be generated to affect the measurements. Analysis of the associated error was given in Section 5.

The current density distribution on the electrode surface was measured by a SVET, with a vibrating amplitude of 30 μm and vibrating frequency of 300 Hz. The steel electrode was either under open-circuit potential or at a cathodic potential of −1.00 V(SCE). The distance between the SVET probe and the steel surface was 200 μm. The SVET measurement was set in a linear scanning mode, with the same designated path as the surface potential measurement.

3. Numerical simulation and analysis

Principally, numerical FE method is able to simulate arbitrarily shaped and sized defects present on the pipe wall, and obtain precise potential and current distributions inside defects. In this work, cylindrical and semi-ellipsoidal ones are chosen since they are more representative of the defects existing on the pipe surface. This provides a promising approach to overcome the experimental difficulty to determine local potential or current density at random positions in a defect.

For FE simulation, the defects were semi-ellipsoidal in shape, rather than the cylindrical shape used in experimental testing, to represent the geometry of corrosion defects in reality, such as those with a stretched crack-shape, pit-shape, and pot-holes as shown in Fig. 4. The width and depth were varied from 0 to 8 mm, and the length was approximately equal to the width for simplification during FE modelling.

The FE simulation was performed through commercial software COMSOL Multiphysics 4.2a. Two physical fields were used in FE modelling, i.e., electrochemical reactions at the steel/solution interface and the potential/current density distributions in solu-

[1] For interpretation of colour in Fig. 1, the reader is referred to the web version of this article.